*Article*

# Electrochemical Detection of Ascorbic Acid in Oranges at MWCNT-AONP Nanocomposite Fabricated Electrode

**Pholoso Calvin Motsaathebe** [1,2] **and Omolola Ester Fayemi** [1,2,*]

1. Department of Chemistry, Faculty of Natural and Agricultural Sciences, Mafikeng Campus, North-West University, Mmabatho 2735, South Africa; pholosocalven@gmail.com
2. Material Science Innovation and Modelling (MaSIM) Research Focus Area, Faculty of Natural and Agricultural Sciences, Mafikeng Campus, North-West University, Mmabatho 2735, South Africa
* Correspondence: Omolola.Fayemi@nwu.ac.za

**Abstract:** Ascorbic acid (AA) is an essential vitamin in the body, influencing collagen formation, as well as norepinephrine, folic acids, tryptophan, tyrosine, lysine, and neuronal hormone metabolism. This work reports on electrochemical detection of ascorbic acid (AA) in oranges using screen-print carbon electrodes (SPCEs) fabricated with multi-walled carbon nanotube- antimony oxide nanoparticle (MWCNT-AONP) nanocomposite. The nanocomposite-modified electrode displayed enhanced electron transfer and a better electrocatalytic reaction towards AA compared to other fabricated electrodes. The current response at the nanocomposite-modified electrode was four times bigger than the bare electrode. The sensitivity and limit of detection (LOD) at the nanocomposite modified electrode was 0.3663 [AA]/$\mu$M and 140 nM, respectively, with linearity from 0.16–0.640 $\mu$M and regression value $R^2$ = 0.985, using square wave voltammetry (SWV) for AA detection. Two well-separated oxidation peaks were observed in a mixed system containing AA and serotonin (5-HT); and the sensitivity and LOD were 0.0224 [AA]/$\mu$A, and 5.85 $\mu$M, respectively, with a concentration range from 23 to 100 $\mu$M ($R^2$ = 0.9969) for AA detection. The proposed sensor outperformed other AA sensors reported in the literature. The fabricated electrode showed great applicability with excellent recoveries ranging from 99 to 107 %, with a mean relative standard deviation (RSD) value of 3.52 % ($n$ = 3) towards detecting AA in fresh oranges.

**Keywords:** ascorbic acid; oranges; electrochemical sensors; nanocomposite; antimony oxide nanoparticles

## 1. Introduction

L-Ascorbic acid (AA) or ascorbate, commonly known as vitamin C, is an important water-soluble vitamin derived from green vegetables, fruits, and other dietary supplements [1]. The role played by AA in the immune defence is extensive [2]. It enables collagen synthesis, which is needed to maintain healthy bones, teeth, skins, cartilages, and stabilization [3]; reduces histamine levels [4]; regulates cytokine synthesis [5]; enhances antibody levels and acts as an antioxidant [6]; reduces necrosis and facilitates apoptosis [7]; improves phagocytosis [8]; and speeds up the wound healing process [9]. In addition, the function of AA as an enzyme co-factor has been established [10,11].

Abnormal AA levels in bodily fluids have been reported to cause cancer, cardiovascular diseases, and Alzheimer's and Parkinson's diseases [12,13]. Extended use of AA could cause urinary oxalate calculus, increase infertility in a woman, and affect embryo development [14]. Furthermore, excessive AA use has been reported to cause diarrhoea, nausea, vomiting, headache, insomnia, gastric irritation, renal problems, loss of food taste, and vomiting. Moreover, excess amounts of AA can act as a peroxidation in the presence of heavy metals such as iron [15].

Although important for their wellbeing, humans, guinea pigs, and other species of birds, fishes, and mammals cannot produce AA. The inability of these aforementioned

species to produce AA is attributed to their evolution over time and specifically the mutation of the L-gulono-lactone oxidase gene, which codes for the enzyme responsible for speeding up the final phase of vitamin C synthesis [16,17]. People obtain their AA supplement from fresh fruits, such as oranges, lemons, mangoes, papayas, strawberries, blackberries, and guava, and vegetables, such as tomatoes, carrots, potatoes, cabbage, and spinach. However, alcohol abuse, drug abuse, ageing, the development of diseases, such as anorexia, and poor diet are among the leading reported causes of reduced AA levels in the body [17,18].

Due to their importance to the food, cosmetic, chemical, and pharmaceutical industries, various analytical methods, such as coulometric [19], high performance liquid chromatography (HPLC) with electrochemical colourimetry [20], electrochemical [21], amperometric [22], capillary electrophoresis [23], gas chromatography [24], and liquid chromatography [25], have been used to determine AA. Nonetheless, most of these analytical methods were found to be less sensitive, expensive, complicated processes and require trained personnel to use them. They require longer sample preparation, are time-consuming; moreover, others need laboratory equipment, except for electrochemical technique [26,27]. Electrochemical sensors fabricated with carbon nanotubes (CNTs), metal oxide nanoparticles, and graphene oxide and conducting polymers have been used extensively to detect AA in different real-life samples [28–35]. These sensors are found to be affordable, offer quick and efficient analysis, and offers highly sensitive and selective.

Nanomaterials have played a critical role in developing affordable, sensitive, and selective sensors [36]. Antimony oxide nanoparticles (AONPs) have found a wide application in the chemical, semi-conducting, and sensing industries due to their unique and exceptional properties, including a high refractive index, high abrasion resistance, high proton conductivity, superior mechanical strength, and high photon absorption capacity [37,38]. They have been used to make flame retardant synergists [39,40], humidity sensors [41], gas sensors [42], light-emitting diodes (LEDs) [43], binary glasses [44], solar cells [45], and anti-friction alloys [46].

The widespread adoption of MWCNTs as electrode modifiers is based on their outstanding and remarkable properties, which include high electrical conductivity, unique mechanical and structural properties [36,47]. CNTs are acid-functionalized to enhance electron transfer and assist with adsorption [48]. CNTs reinforced with metal oxide nanoparticles nanocomposite fabricated electrodes are increasingly being investigated due to improved electrical, magnetic, and optical properties resulting from synergies between two nanomaterials [49,50].

Apinya et al. [51] developed a polyaniline/$MnO_2$-$Sb_2O_3$ nanocomposite sensor to detect AA and acetylsalicylic acid (ASA) in human urine. Using the differential pulse voltammetry (DPV) technique, their sensors demonstrated sensitivity and LOD values of 0.9356 nmol $L^{-1}$ and 0.071 nmol $L^{-1}$, respectively, with a concentration range within 0.1–372.64 nmol $L^{-1}$ ($R^2$ = 0.9974). In the same vein, Şehriban et al. [52] used the SWV technique to determine metaproterenol from biological and pharmaceutical materials using AONP-$WO_3$-CNTs@GCE. Their electrode displayed a linear range and LOD of 52–270 nM for metaproterenol detection and 6.6 nM. Similarly, Masibi et al. [53,54] used MWCNT-AONP-PANI@GCE to detect endosulfan, and lindane, respectively, from water samples via the SWV method.

No research paper in the literature discusses the determination of AA in tomatoes using AONP-MWCNT nanocomposite electrodes. Therefore, this paper discusses the detection of AA at nanocomposite by employing cyclic voltammetry and square wave techniques. The fabricated sensors displayed enhanced electrocatalytic and electroanalytic properties towards detecting AA. The synergistic effect of the two nanomaterials resulted in faster electron transfer kinetics at the electrode.

## 2. Reagents and Experimental Procedure

### 2.1. Reagents

The following chemicals were purchased and used as received from the manufacturers, serotonin (5-HT) hydrochloride powder (98%), antimony trichloride (99%) (SbCl$_3$), ascorbic acid (AA) (99%), hydrochloric acid (32%) (HCL), sodium hydroxide (NaOH) (98%), multi-walled carbon nanotubes abbreviated MWCNTs ($\geq$98%), N, N-dimethylformamide (C$_3$H$_7$NO) (99%), nitric acid (HNO$_3$) (34%), and toluene (C$_7$H$_8$) (99%) were obtained from Merck Pty Ltd. (Darmstadt, Germany). Sodium phosphate salts Na$_2$HPO$_4$ (99%) and NaH$_2$PO$_4$ (99%) products of LABCHEM and GlassWorld, located in Johannesburg, South africa were used in the preparation of 0.1 M phosphate buffer solution (PBS) at pH 7. Emplura® Merck (The Chemical Center from Mumbai, India) provided distilled water, which was used through the experiment to prepare chemicals.

### 2.2. Antimony Oxide Nanoparticles (AONPs) Synthetic Method

The synthetic method followed to synthesis antimony oxide nanoparticles (AONPs) was adopted from Chen et al. [55]. A colourless solution was prepared by dissolving 2 mM antimony trichloride in toluene under rapid stirring for 15 min. Then, 20 mL of distilled water was added to create a lacteous colloid. Then the solution was re-adjusted to a pH of 8–9 by adding 6 M NaOH. It was then agitated for an additional 20 min and then placed in a stainless-steel autoclave with Teflon-lined walls for 12 h at 120 °C. The formed product was washed with distilled water and ethanol several times and then dried in an oven at 60 °C for 6 h.

### 2.3. Synthesis of f-MWCNTs

The nitric acid treatment approach synthesized functionalized multi-walled carbon nanotubes (f-MWCNTs). In 1 M nitric acid, about 300 mg of raw multi-walled carbon nanotubes (r-MWCNTs) was dissolved. After that, the mixture was sonicated in cold water at 50 °C for 240 min. The mixture was then filtered with deionized water until a pH 7 was reached. The finished product was dried in an oven overnight [56].

### 2.4. MWCNT-AONP Nanocomposite Synthesis

About 2 mg f-MWCNTs and 6 mg AONPs were dissolved into 2 mL dimethylformamide (DMF) with continuous stirring at room temperature for 48 h. The resultant AONP-MWCNT nanocomposite was dried at 25 °C in an oven for 24 h [55].

### 2.5. Real-Sample Analysis

The applicability of the fabricated electrode to detect AA in a real sample was examined using fresh oranges bought from a nearby supermarket. The oranges were crushed to extract their juice and filtered using Whatman No 1 filter paper to obtain an AA extract solution. A fixed volume of the oranges extract (1 mL) was added to different volumes of the stock solution to make up to 10 mL of the sample. The experiment was done in triplicates using SWV.

## 3. Results and Discussion

### 3.1. Electrocatalytic Experiements

The comparative cyclic voltammogram between bare and modified screen printed carbon electrodes (SPCEs) in 0.1 mM AA is shown in Figure 1. The voltammograms in Figure 1a indicate that the reactions of AA at the electrodes were irreversible; also, modified electrodes showed enhanced cyclic voltammogram shapes compared to bare electrodes. The voltammogram in Figure 1a,b showed a decrease in AA current response in the following order: SPCE-AONP-MWCNT (Ipa = 60.71 µA; Epa = 0.032 V), SPCE-AONPs (Ipa = 11.36 µA; Epa = 0.034 V), and SPCE-bare (Ipa = 14.96 µA; Epa = 0.45 V). The Epa value of 0.032 V at the nanocomposite modified electrode matched with other studies from the literature [28,29,57], while the SPCE/f-MWCNTs did not interact with AA. A higher current response noted at the

nanocomposite electrode was attributed to the synergic effect between the two nanomaterials. Figure 1c shows a scan rate study at the proposed sensor with a scan rate of 10–350 mVs$^{-1}$. According to Figure 1d, a diffusion-controlled reaction was based on a linear relationship against peak current vs. square root. The linear relationship between Ipa vs $v^{1/2}$ can be expressed with this equation: Ipa = 44.143 $v^{1/2}$ − 135.55 (R$^2$ = 0.9930). A detailed description of the electrooxidation mechanism pathway of AA is provided by Scheme 1.
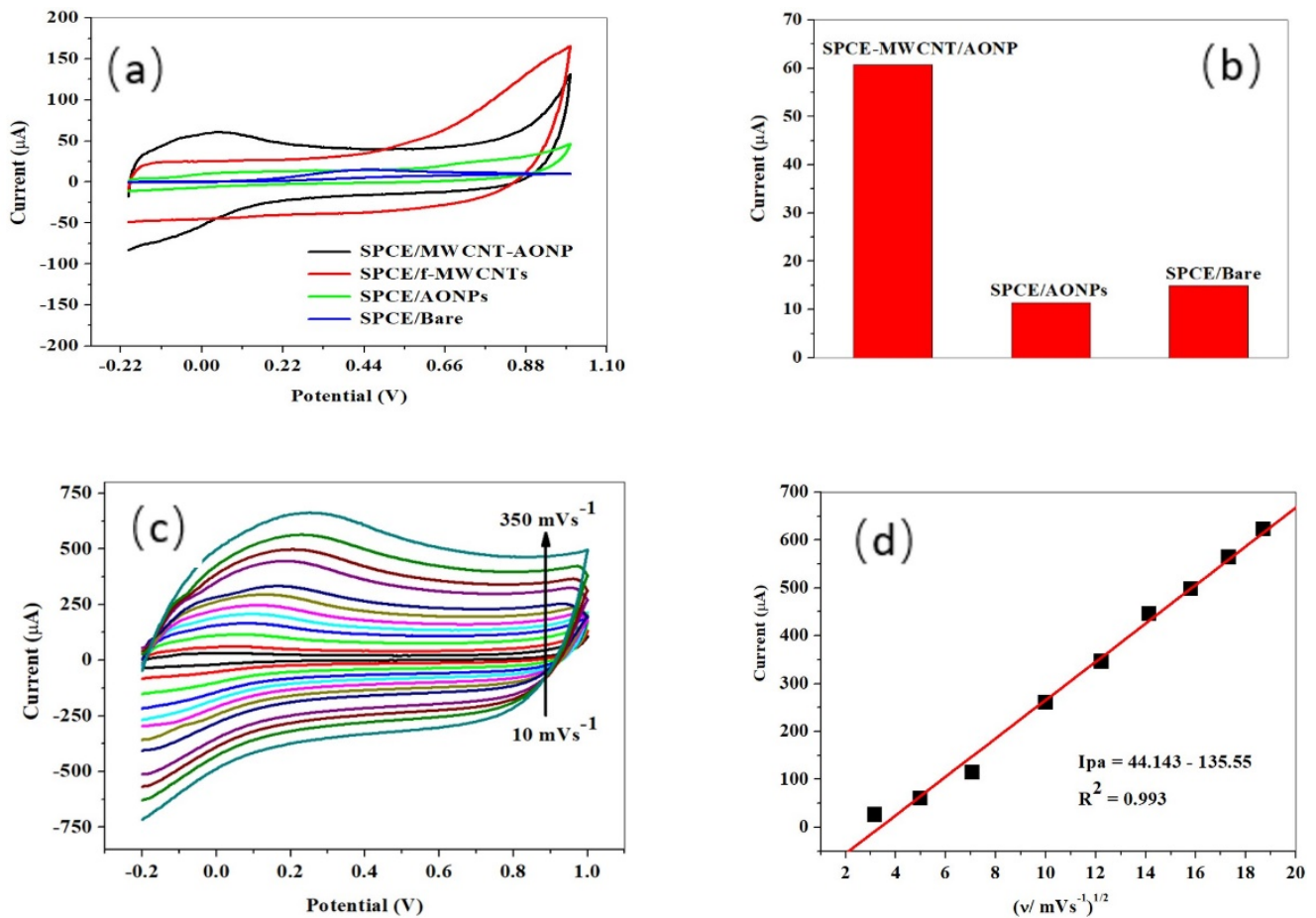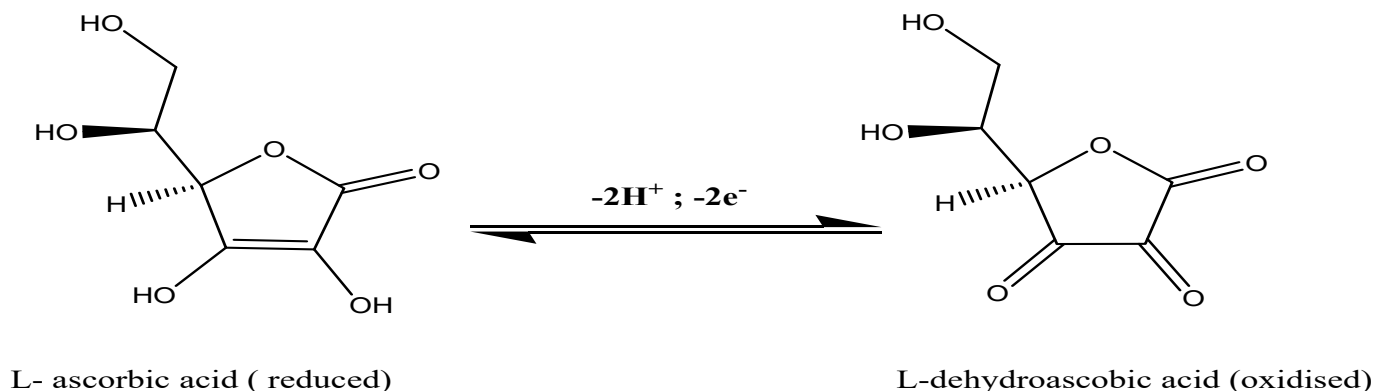


**Figure 1.** Comparative cyclic voltammograms at modified and bare electrode for (**a**) AA detection, (**b**) comparative currents response between bare and modified electrode, (**c**) scan rate study (10–350 mVs$^{-1}$), and (**d**) shows a linear relationship between Ipa vs. $v^{1/2}$.



L- ascorbic acid ( reduced)　　　　　　　　　L-dehydroascobic acid (oxidised)

**Scheme 1.** AA redox mechanism pathway.

### 3.2. Electro-Analytic Experiments

Figure 2a,b depicts a linear relationship between peak current and increasing AA (0.040–0.640 µM) concentration. For AA detection, the sensitivity, LOD, and limit of quantification (LOQ) was 0.3663 [AA]/µA, 140 nM, and 423 nM, respectively, with concentration range from $4 \times 10^{-8}$–$6.4 \times 10^{-7}$ M ($R^2 = 0.9851$). As shown in Table 1, the proposed sensor performed better than other AA electrochemical sensors from the literature. The synergy between MWCNTs and AONPs in facilitating electron transfer cannot be overstated. Similarly, the MWCNTs are an essential component of the nanocomposite electrode's outstanding performance. Its wide surface area allows free passage of electrolytes and charges between the base electrode and electroactive species on the electrode surface. The conductive properties of the AONPs and MWCNTs and the ionic interaction between the two nanomaterials are some of the mechanisms responsible for this considerable electron transport at the fabricated electrode. Using Equations (1) and (2), the suggested electrode's resulting LOD, and LOQ values were computed. The results suggest that the constructed sensors detect AA at low concentrations with excellent sensitivity and reliability.

$$\text{LOD} = \frac{3.3 \times SD}{s}, \tag{1}$$

$$\text{LOQ} = \frac{10 \times SD}{s}, \tag{2}$$

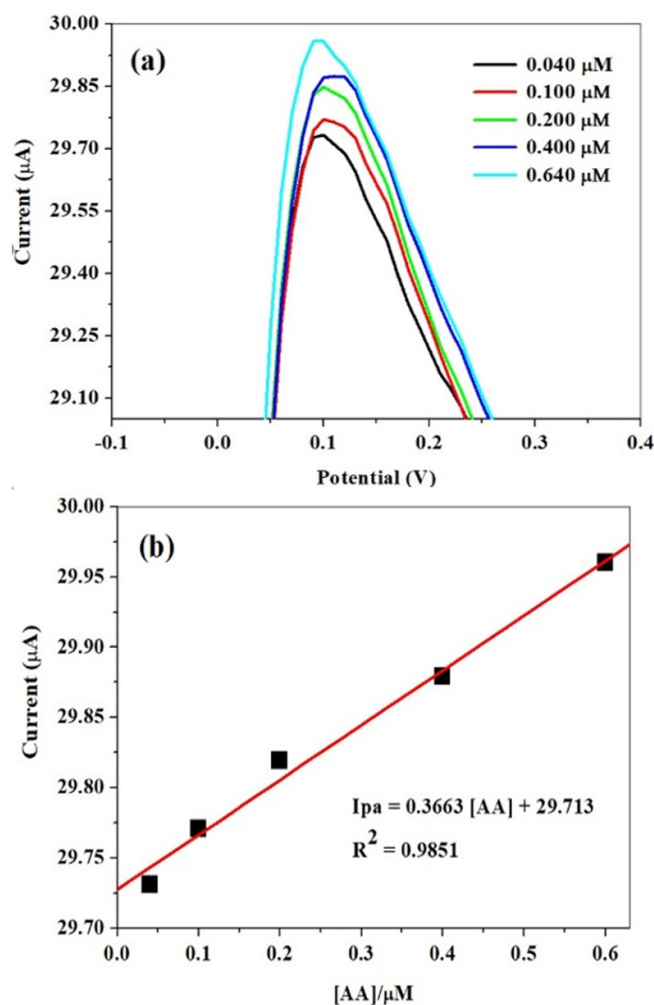*SD* stands for standard deviation, while *s* stands for gradient slope.



**Figure 2.** (**a**) AA detection within the 0.16–0.640 µM linear range, and (**b**) corresponding linear plots.

**Table 1.** List of AA electrochemical sensors from literature.

| Modified Electrode | Method | Linearity (µM) | LOD (µM) | R² | Ref |
|---|---|---|---|---|---|
| [1] PVP-GR/GCE | LSV | 4.0–1000 | 0.80 | 0.989 | [58] |
| RGO–ZnO/GCE | DPV | 50–2350 | 3.71 | 0.997 | [35] |
| Sonigel-carbon@ME | SWV | 50–1000 | 50.0 | 0.995 | [59] |
| [2] CF/ZnO CN-ME | DPV | 0.6–1800 | 156.7 | 0.992 | [60] |
| [3] ITO-rGO-AuNPs | LSV | 20–100 | 5.63 | 0.996 | [61] |
| Fe₃O₄NPs@SPCE | SWV | 10–100 | 15.7 | 0.981 | [57] |
| MWCNT-AONP@SPCE | SWV | 0.04–0.64 | 0.14 | 0.985 | This work |

[1] Glassy carbon electrode modified with a polyvinylpyrrolidone (PVP)-graphene composite film (PVP-GR/GCE); [2] Carbon fibers/ZnO coaxial nanocable microelectrode; [3] Reduced graphene oxide incorporated with gold nanoparticles modified on indium tin oxide (ITO) electrodes.

### 3.3. Simultaneous Detection of AA and 5-HT

Figure 3a shows simultaneous detection of AA (23–100 µM) in the presence of 0.5 mM 5-HT. The AA current response increased linearly with increasing AA concentration while the 5-HT peak current remained constant. It was evident that the proposed sensor has excellent anti-interference performance, as evidenced by two visible well-separated peaks located at 0.038 V and 0.350 V representing AA and 5-HT, respectively, as well as a 360 mV potential peak separation between AA- 5-HT as displayed in Figure 3c. Figure 3b shows corresponding calibration plots for AA. For detection of AA in presences of 0.5 mM 5-HT, the sensitivity, LOD, and LOQ at the modified electrode were 0.0224 [AA]/µA, 5.85 µM, and 19.51 µM, respectively, with a linear ranging from 23–100 µM (R² = 0.9969) utilizing SWV.



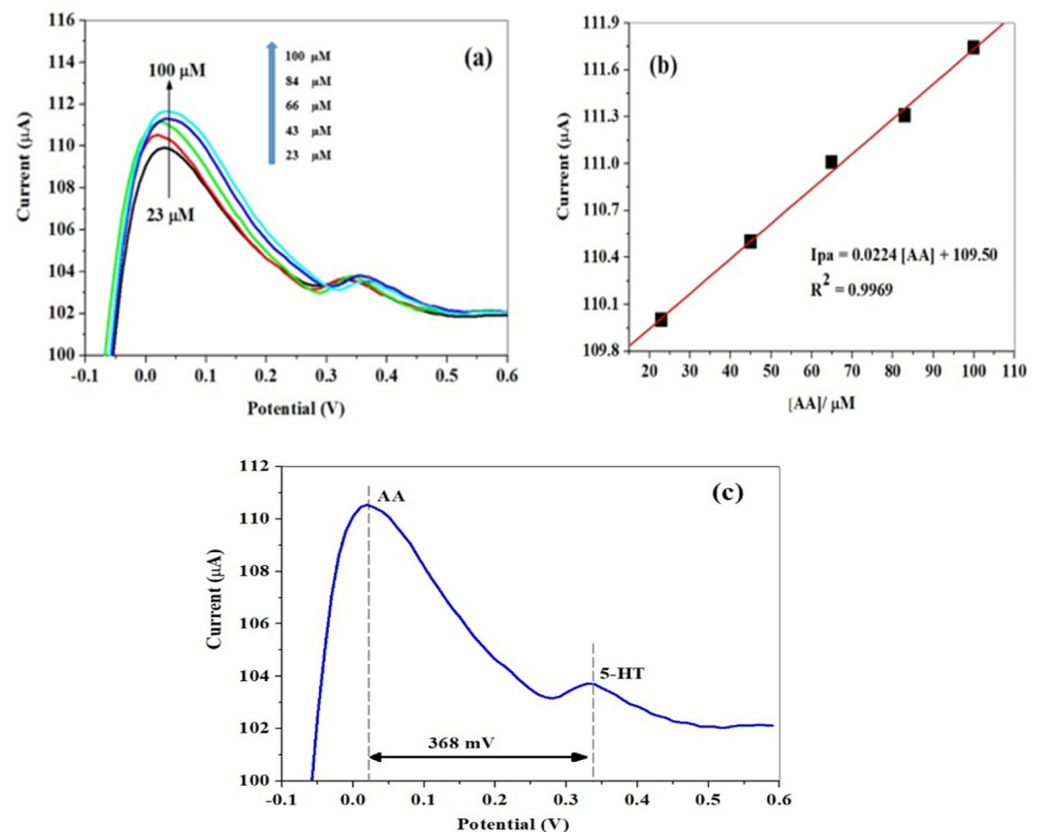**Figure 3.** (**a**) Detection of AA from 23 to 100 µM concentration range in the presence of 0.5 mM 5-HT, (**b**) corresponding linear curves, and (**c**) simultaneous detection of 0.5 mM (AA and 5-HT) at the proposed electrode.

### 3.4. Reproducibility and Shelve-Life Study of The Proposed Sensor

This experiment aimed to test the feasibility and re-usability of the constructed sensor. Using the CV technique, the experiment was repeated (20 times) in 0.1 mM AA at a scan rate of 25 mVs$^{-1}$. The anodic peak decreased by 42%, and the electrode showed an RSD value of 20% towards the detection of AA, as shown in Figure 4a. A decrease in the AA peak current might be attributed to more nanocomposite (SPCE-MWCNT-AONP) assimilation into the electrode surface over time. Figure 4b shows the results of the repeatability study at the suggested electrode for four weeks using the cyclic voltammetry (CV) method. The constructed sensor was stored in a dry environment when not in use. The electrode maintained an acceptable AA current response for 4 weeks, indicating the proposed sensor's longevity.
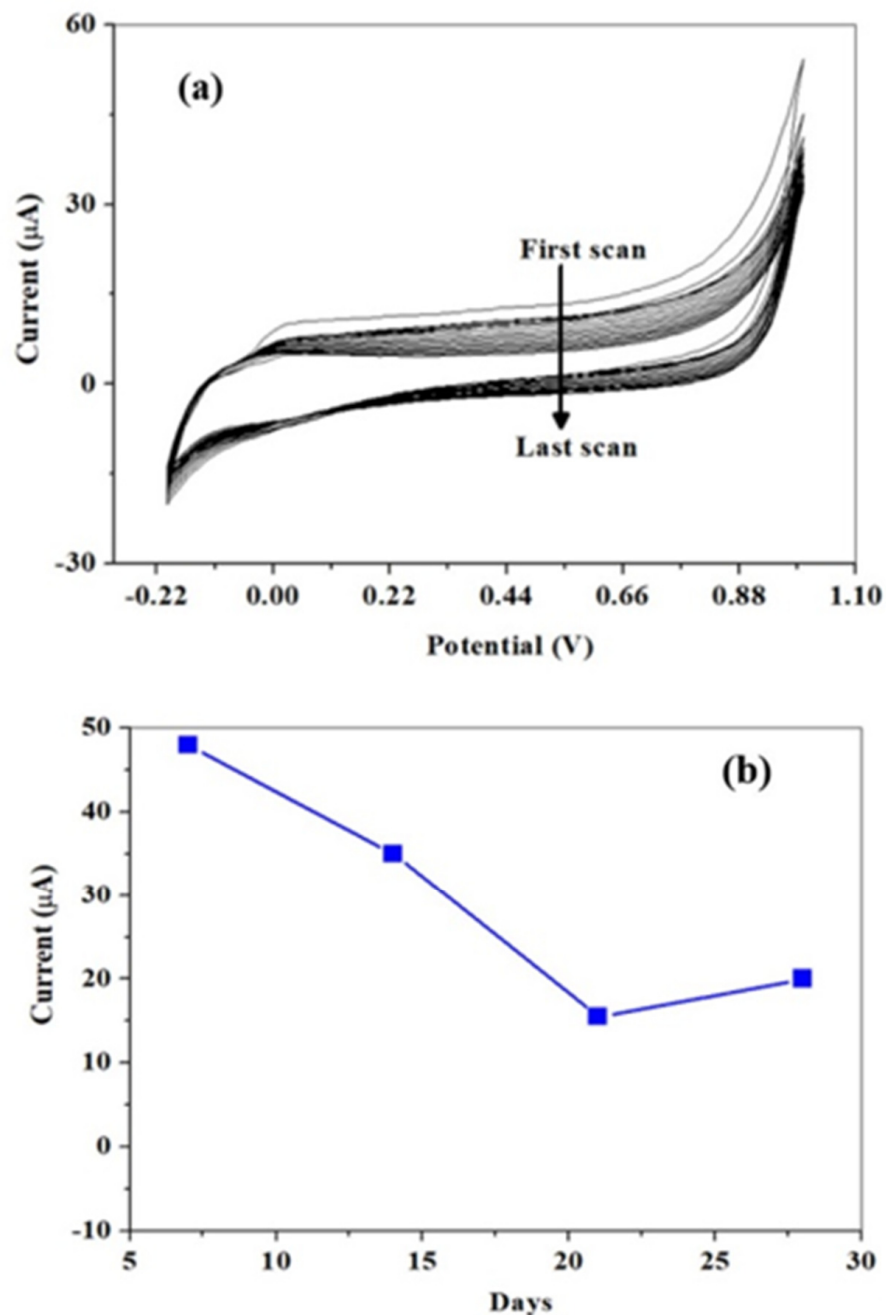


**Figure 4.** (**a**) Reproducibility study and (**b**) shelve-life study carried out at the constructed sensor.

*3.5. Real-Aample Analysis*

The proposed electrode displayed excellent recoveries ranging from 99.12 to 107.76%, with an average RSD (%) value of 3.52 (*n* = 3) for detecting AA in oranges. The results of the experiment are summarised in Table 2. The % recovery was calculated utilizing Equation (3).

$$\% \text{ Recovery} = \frac{\text{quantity found} - \text{quantity detected}}{\text{quantity added}} \tag{3}$$

**Table 2.** Detection of AA in fresh oranges.

| Sample | Added (μM) | Detected (μM) | Recovery (%) | RSD (%) |
|--------|-----------|---------------|--------------|---------|
| Oranges | 400 | 431.03 | 107.76 | 5.71 |
| | 600 | 594.69 | 99.12 | 3.89 |
| | 900 | 919.52 | 102.17 | 0.97 |

*n* = 3; average RSD (%) = 3.52.

**4. Conclusions**

This study has finalized the development of an electrochemical sensor fabricated with AONP-MWCNT on SPCEs to detect AA in tomatoes. The nanocomposite electrode displayed greater electrocatalytic activity toward AA with respect to other electrodes. The reactions of AA are diffusion-controlled and irreversible at the nanocomposite electrode. For AA detection, the proposed sensor electrode displayed sensitivity, LOD, and LOQ values of 0.4789 μA/μM, 278 nM, and 842 nM, respectively, with linearity from 0.16 to 0.640 μM ($R^2$ = 0.9851) using SWV. For simultaneous detection of AA in the presences of 0.5 mM 5-HT, the electrode displayed the sensitivity, LOD, and LOQ as 0.0224 μA/μM, 5.85 μM, 19.51 μM, respectively, with linearity from 23 to 100 μM ($R^2$ = 0.9969). The fabricated sensor exhibited excellent anti-interference behaviour and long shelve life. A sensor based on the proposed design was successfully applied to detecting AA in oranges, showing remarkable recovery rates exceeding 99.12% with a 3.52% relative standard deviation (RSD). The proposed sensor is highly selective, simple to use, inexpensive, quick, and offers accurate analysis. Therefore, this sensor could potentially be used to detect other important analytes such as neurotransmitters, organochlorides (pesticides and herbicides), and vitamins, etc. For future studies, a binder or electrode stabilizers could be used to improve the stability of the proposed sensor.

**References**

1. Fadhel, D.H. Spectrophotometric determination of ascorbic acid in aqueous solutions. *Al-Nahrain J. Sci.* **2012**, *15*, 88–94. [CrossRef]
2. Carr, A.C.; Maggini, S. Vitamin C and immune function. *Nutrients* **2017**, *9*, 1211. [CrossRef] [PubMed]
3. Tajima, S.; Pinnell, S.R. Ascorbic acid preferentially enhances type I and III collagen gene transcription in human skin fibroblasts. *J. Dermatol. Sci.* **1996**, *11*, 250–253. [CrossRef]

4.  Johnston, C.S.; Huang, S. Effect of ascorbic acid nutriture on blood histamine and neutrophil chemotaxis in guinea pigs. *J. Nutr.* **1991**, *121*, 126–130. [CrossRef] [PubMed]
5.  Mohammed, B.M.; Fisher, B.J.; Kraskauskas, D.; Farkas, D.; Brophy, D.F.; Natarajan, R. Vitamin C: A novel regulator of neutrophil extracellular trap formation. *Nutrients* **2013**, *5*, 3131–3150. [CrossRef]
6.  Stankova, L.; Gerhardt, N.B.; Nagel, L.; Bigley, R.H. Ascorbate and phagocyte function. *Infect. Immun.* **1975**, *12*, 252–256. [CrossRef]
7.  Sharma, P.; Raghavan, S.A.; Saini, R.; Dikshit, M. Ascorbate-mediated enhancement of reactive oxygen species generation from polymorphonuclear leukocytes: Modulatory effect of nitric oxide. *J. Leukoc. Biol.* **2004**, *75*, 1070–1078. [CrossRef]
8.  Ganguly, R.; Durieux, M.; Waldman, R.J. Macrophage function in vitamin C-deficient guinea pigs. *Am. J. Clin. Nutr.* **1976**, *29*, 762–765. [CrossRef]
9.  Desneves, K.J.; Todorovic, B.E.; Cassar, A.; Crowe, T.C. Treatment with supplementary arginine, vitamin C and zinc in patients with pressure ulcers: A randomised controlled trial. *Clin. Nutr.* **2005**, *24*, 979–987. [CrossRef]
10. Chauhan, N.; Soni, S.; Agrawal, P.; Balhara, Y.P.S.; Jain, U. Recent advancement in nanosensors for neurotransmitters detection: Present and future perspective. *Process Biochem.* **2020**, *91*, 241–259. [CrossRef]
11. Gupta, P.; Tiwari, S.; Haria, J. Relationship between depression and vitamin C status: A study on rural patients from western uttar pradesh in India. *Int. J. Sci. Study* **2014**, *1*, 37–39.
12. Manjunatha, J.G.; Swamy, B.K.; Deraman, M.; Mamatha, G.P. Simultaneous determination of ascorbic acid, dopamine and uric acid at poly (aniline blue) modified carbon paste electrode: A cyclic voltammetric study. *Int. J. Pharm. Pharm. Sci.* **2013**, *5*, 355–362.
13. Pisoschi, A.M.; Pop, A.; Serban, A.I.; Fafaneata, C. Electrochemical methods for ascorbic acid determination. *Electrochim. Acta* **2014**, *121*, 443–460. [CrossRef]
14. Guo, X.; Yue, G.; Huang, J.; Liu, C.; Zeng, Q.; Wang, L. Label-free simultaneous analysis of Fe (III) and ascorbic acid using fluorescence switching of ultrathin graphitic carbon nitride nanosheets. *ACS Appl. Mater. Interfaces* **2018**, *10*, 26118–26127. [CrossRef] [PubMed]
15. Hodkinson, A. *Oxalic Acid in Biology and Medicine*; Academic Press: London, UK, 1977; pp. 254–319.
16. Drouin, G.; Godin, J.R.; Pagé, B. The genetics of vitamin C loss in vertebrates. *Curr. Genom.* **2011**, *12*, 371–378. [CrossRef] [PubMed]
17. Elgailani, I.E.H.; Elkareem, M.; Noh, E.; Adam, O.; Alghamdi, A. Comparison of two methods for the determination of vitamin C (ascorbic acid) in some fruits. *Am. J. Chem.* **2017**, *2*, 1–7. [CrossRef]
18. Vissers, M.C.; Carr, A.C.; Pullar, J.M.; Bozonet, S.M. The bioavailability of vitamin C from kiwifruit. *Adv. Food Nutr. Res.* **2013**, *68*, 125–147.
19. Kyaw, A. A simple colorimetric method for ascorbic acid determination in blood plasma. *Clin. Chim. Acta* **1978**, *86*, 153–157. [CrossRef]
20. Washko, P.W.; Hartzell, W.O.; Levine, M. Ascorbic acid analysis using high-performance liquid chromatography with coulometric electrochemical detection. *Anal. Biochem.* **1989**, *181*, 276–282. [CrossRef]
21. Badea, M.; Florescu, M.; Veregut, V.; Chelmea, L.; Corcan, O.; Floroian, L.; Restani, P.; Marty, J.; Moga, M. Optimization of electrochemical detection of L-ascorbic acid from plant food supplements using screen printed transducers. *Adv. Anal. Chem.* **2015**, *5*, 69–73.
22. De Faria, L.V.; Lisboa, T.P.; de Farias, D.M.; Araujo, F.M.; Machado, M.M.; de Sousa, R.A.; Matos, M.A.C.; Muñoz, R.A.A.; Matos, R.C. Direct analysis of ascorbic acid in food beverage samples by flow injection analysis using reduced graphene oxide sensor. *Food Chem.* **2020**, *319*, 126509. [CrossRef] [PubMed]
23. Versari, A.; Mattioli, A.; Parpinello, G.P.; Galassi, S. Rapid analysis of ascorbic and isoascorbic acids in fruit juice by capillary electrophoresis. *Food Control* **2004**, *15*, 355–358. [CrossRef]
24. Silva, F.O. Total ascorbic acid determination in fresh squeezed orange juice by gas chromatography. *Food Control* **2005**, *16*, 55–58. [CrossRef]
25. Oliveira, E.J.; Watson, D.G. Chromatographic techniques for the determination of putative dietary anticancer compounds in biological fluids. *J. Chromatogr. B Biomed. Sci. Appl.* **2001**, *764*, 3–25. [CrossRef]
26. Habibi, B.; Jahanbakhshi, M.; Pournaghi-Azar, M.H. Differential pulse voltammetric simultaneous determination of acetaminophen and ascorbic acid using single-walled carbon nanotube-modified carbon–ceramic electrode. *Anal. Biochem.* **2011**, *411*, 167–175. [CrossRef]
27. López-Pastor, J.A.; Martínez-Sánchez, A.; Aznar-Poveda, J.; García-Sánchez, A.J.; García-Haro, J.; Aguayo, E. Quick and Cost-Effective Estimation of Vitamin C in Multifruit Juices Using Voltammetric Methods. *Sensors* **2020**, *20*, 676. [CrossRef]
28. Aryal, K.P.; Jeong, H.K. Electrochemical detection of ascorbic acid with chemically functionalized carbon nanofiber/beta-cyclodextrin composite. *Chem. Phys. Lett.* **2020**, *757*, 137881. [CrossRef]
29. Das, T.R.; Sharma, P.K. Hydrothermal-assisted green synthesis of Ni/Ag@rGO nanocomposite using Punica granatum juice and electrochemical detection of ascorbic acid. *Microchem. J.* **2020**, *156*, 104850. [CrossRef]
30. Fernandes, D.S.; do Carmo, D.R. Silsesquioxane Modified with PAMAM Dendrimer and a Bimetallic Complex for Electrochemical Detection of Ascorbic Acid. *Electroanalysis* **2020**, *33*, 365–374. [CrossRef]
31. Gai, P.; Zhang, H.; Zhang, Y.; Liu, W.; Zhu, G.; Zhang, X.; Chen, J. Simultaneous electrochemical detection of ascorbic acid, dopamine and uric acid based on nitrogen doped porous carbon nanopolyhedra. *J. Mater. Chem. B* **2013**, *1*, 2742–2749. [CrossRef]

32. Ibarlucea, B.; Roig, A.P.; Belyaev, D.; Baraban, L.; Cuniberti, G. Electrochemical detection of ascorbic acid in artificial sweat using a flexible alginate/CuO-modified electrode. *Microchim. Acta* **2020**, *187*, 1–11. [CrossRef] [PubMed]

33. Park, S.G.; Park, J.E.; Cho, E.I.; Hwang, J.H.; Ohsaka, T. Electrochemical detection of ascorbic acid and serotonin at a boron-doped diamond electrode modified with poly(N,N-dimethylaniline). *Res. Chem. Intermed.* **2006**, *32*, 595–601. [CrossRef]

34. Sun, C.L.; Lee, H.H.; Yang, J.M.; Wu, C.C. The simultaneous electrochemical detection of ascorbic acid, dopamine, and uric acid using graphene/size-selected Pt nanocomposites. *Biosens. Bioelectron.* **2011**, *26*, 3450–3455. [CrossRef] [PubMed]

35. Zhang, X.; Zhang, Y.-C.; Ma, L.X. One-pot facile fabrication of graphene-zinc oxide composite and its enhanced sensitivity for simultaneous electrochemical detection of ascorbic acid, dopamine and uric acid. *Sens. Actuators B Chem.* **2016**, *227*, 488–496. [CrossRef]

36. Zestos, A.G. Carbon nanoelectrodes for the electrochemical detection of neurotransmitters. *Int. J. Electrochem.* **2018**, *2018*, 3679627. [CrossRef]

37. Chang, P.R.; Yu, J.; Ma, X.J.M.M. Fabrication and characterization of $Sb_2O_3$/carboxymethyl cellulose sodium and the properties of plasticized starch composite films. *Macromol. Mater. Eng.* **2009**, *294*, 762–767. [CrossRef]

38. Falcaro, P.; Ricco, R.; Yazdi, A.; Imaz, I.; Furukawa, S.; Maspoch, D.; Ameloot, R.; Evans, J.D.; Doonan, C. Application of metal and metal oxide nanoparticles@ MOFs. *Coord. Chem. Rev.* **2016**, *307*, 237–254. [CrossRef]

39. Karak, N.; Maiti, S. Antimony polymers. III. Flame retardant behavior of chloroprene and natural rubber vulcanizates with antimony polymer. *J. Appl. Polym. Sci.* **1998**, *68*, 927–935. [CrossRef]

40. Mostashari, S.; Baie, S. Thermogravimetry studies of cotton fabric's flame-retardancy by means of synergism of lithium bromide and antimony trioxide. *J. Therm. Calorim.* **2008**, *94*, 97–101. [CrossRef]

41. Miura, N.; Mizuno, H.; Yamazoe, N.J. Humidity sensor using antimony phosphate operative at a medium temperature of 150–250 °C. *Jpn. J. Appl. Phys.* **1988**, *27*, L931. [CrossRef]

42. Badawy, W.; El-Taher, E.A. Preparation and electrochemical behaviour of some metal oxide films. *Thin Solid Films* **1988**, *158*, 277–284. [CrossRef]

43. Sahoo, N.K.; Apparao, K.V. Process-parameter optimization of $Sb_2O_3$ films in the ultraviolet and visible region for interferometric applications. *Appl. Phys. A* **1996**, *63*, 195–202. [CrossRef]

44. El-Diasty, F.; Wahab, F.A.; Abdel-Baki, M. Optical band gap studies on lithium aluminum silicate glasses doped with $Cr^{3+}$ ions. *J. Appl. Phys.* **2006**, *100*, 093511. [CrossRef]

45. Tigau, N.; Ciupina, V.; Prodan, G. The effect of substrate temperature on the optical properties of polycrystalline $Sb_2O_3$ thin films. *J. Cryst. Growth* **2005**, *277*, 529–535. [CrossRef]

46. Chin, H.S.; Cheong, K.Y.; Razak, K.A. Review on oxides of antimony nanoparticles: Synthesis, properties, and applications. *J. Mater. Sci.* **2010**, *45*, 5993–6008. [CrossRef]

47. Wang, Z.H.; Liang, Q.l.; Wang, Y.M.; Luo, G.A. Carbon nanotube-intercalated graphite electrodes for simultaneous determination of dopamine and serotonin in the presence of ascorbic acid. *J. Electroanal. Chem.* **2003**, *540*, 129–134. [CrossRef]

48. McCreery, R.L. Advanced carbon electrode materials for molecular electrochemistry. *Chem. Rev.* **2008**, *108*, 2646–2687. [CrossRef]

49. Li, G.; Xia, Y.; Tian, Y.; Wu, Y.; Liu, J.; He, Q.; Chen, D. Recent developments on graphene-based electrochemical sensors toward nitrite. *J. Electrochem. Soc.* **2019**, *166*, B881. [CrossRef]

50. Saleh, T.A.; Siddiqui, M.N.; Al-Arfaj, A.A. Synthesis of multi-walled carbon nanotubes-titania nanomaterial for desulfurization of model fuel. *J. Nanomater.* **2014**, *2014*, 194. [CrossRef]

51. Puangjan, A.; Chaiyasith, S.; Wichitpanya, S.; Daengduang, S.; Puttota, S. Electrochemical sensor based on PANI/$MnO_2$-$Sb_2O_3$ nanocomposite for selective simultaneous voltammetric determination of ascorbic acid and acetylsalicylic acid. *J. Electroanal. Chem.* **2016**, *782*, 192–201. [CrossRef]

52. Düzmen, Ş.; Aslanoglu, M. An electrochemical platform of bimetallic oxide ($Sb_2O_3$@ $WO_3$) nanoparticles and carbon nanotubes for the sensitive determination of metaproterenol in pharmaceuticals and biological samples. *Measurement* **2021**, *173*, 108572. [CrossRef]

53. Masibi, K.K.; Fayemi, O.E.; Adekunle, A.S.; Al-Mohaimeed, A.M.; Fahim, A.M.; Mamba, B.B.; Ebenso, E.E. Electrochemical detection of endosulfan using an AONP-PANI-SWCNT modified glassy carbon electrode. *Materials* **2021**, *14*, 723. [CrossRef] [PubMed]

54. Masibi, K.K.; Fayemi, O.E.; Adekunle, A.S.; Sherif, E.M.; Ebenso, E.E. Electrocatalysis of Lindane Using Antimony Oxide Nanoparticles Based-SWCNT/PANI Nanocomposites. *Front. Chem.* **2018**, *6*, 423. [CrossRef] [PubMed]

55. Chen, X.; Huh, H.; Lee, S.W. Hydrothermal synthesis of antimony oxychloride and oxide nanocrystals: $Sb_4O_5Cl_2$, $Sb_8O_{11}Cl_2$, and $Sb_2O_3$. *J. Solid State Chem.* **2008**, *181*, 2127–2132. [CrossRef]

56. Ba Hashwan, S.S.; Fatin, M.; Ruslinda, A.R.; Md Arshad, M.; Hashim, U.; Ayub, R. Functionalization of Multi Wall Carbon Nanotubes Using Nitric Acid Oxidation. *Appl. Mech. Mater.* **2015**, *754–755*, 1156–1160. [CrossRef]

57. Uwaya, G.E.; Fayemi, O.E. Electrochemical Detection of Ascorbic acid in Orange on Iron (III) Oxide Nanoparticles Modified Screen Printed Carbon Electrode. *J. Clust. Sci.* **2021**, *32*, 1–9. [CrossRef]

58. Wu, Y.; Deng, P.; Tian, Y.; Feng, J.; Xiao, J.; Li, J.; Liu, J.; Li, G.; He, Q. Simultaneous and sensitive determination of ascorbic acid, dopamine and uric acid via an electrochemical sensor based on PVP-graphene composite. *J. Nanobiotechnol.* **2020**, *18*, 1–13. [CrossRef]

59. Choukairi, M.; Bouchta, D.; Bounab, L.; Elkhamlichi, R.; Chaouket, F.; Raissouni, I.; Rodriguez, I. Electrochemical detection of uric acid and ascorbic acid: Application in serum. *J. Electroanal. Chem.* **2015**, *758*, 117–124. [CrossRef]

60. Gu, B.; Liu, Z.; Wang, X.; Dong, X. RF magnetron sputtering synthesis of carbon fibers/ZnO coaxial nanocable microelectrode for electrochemical sensing of ascorbic acid. *Mater. Lett.* **2016**, *181*, 265–267. [CrossRef]

61. Mazzara, F.; Patella, B.; Aiello, G.; O'Riordan, A.; Torino, C.; Vilasi, A.; Inguanta, R. Electrochemical detection of uric acid and ascorbic acid using r-GO/NPs based sensors. *Electrochim. Acta* **2021**, *388*, 138652. [CrossRef]